Self-Supervised Convolutional Subspace Clustering Network

Anonymous CVPR submission

Paper ID 3260

Abstract

Subspace clustering methods based on data self-expressiveness have become very popular for learning from data that lie in a union of low-dimensional linear subspaces. However, in the absence of proper feature extraction, the applicability of subspace clustering has been restricted because practical visual data in raw form do not necessarily lie in such linear structures. On the other hand, while Convolutional Neural Network (ConvNet) has been demonstrated as a powerful tool for feature extraction from visual data, training such a ConvNet usually requires a large amount of labeled data, which are unavailable in subspace clustering applications. To achieve simultaneously feature learning and subspace clustering, we propose an end-to-end trainable framework called the Self-Supervised Convolutional Subspace Clustering Network (S^{2}ConvSCN) that combines a ConvNet module (for feature learning), a self-expression module (for subspace clustering) and a spectral clustering module (for self-supervision) into a joint optimization framework. Particularly, we introduce a dual self-supervision that exploits the output of spectral clustering to supervise the training of the feature learning module (via a classification loss) and the self-expression module (via a spectral clustering loss). Our experiments on four benchmark datasets show the effectiveness of the dual self-supervision and demonstrate superior performance of our proposed approach.

1. Introduction

In many real-world applications such as image and video processing, we need to deal with a large amount of high-dimensional data. Such data can often be well approximated by a union of multiple low-dimensional subspaces, where each subspace corresponds to a class or a category. For example, the frontal facial images of a subject taken under varying lighting conditions approximately span a linear subspace of dimension up to nine [10]; the trajectories of feature points related to a rigidly moving object in a video sequence span an affine subspace of dimension up to three [39]; the set of handwritten digit images of a single digit also approximately span a low-dimensional subspace [7]. In such cases, it is important to segment the data into multiple groups where each group contains data points from the same subspace. This problem is known as *subspace clustering* [40], which we formally define as follows.

Problem (Subspace Clustering). *Let $X \in \mathbb{R}^{D\times N}$ be a real-valued matrix whose columns are drawn from a union of n subspaces of $\mathbb{R}^D$, $\bigcup_{i=1}^{n}\{S_i\}$, of dimensions $d_i \ll \min\{D, N\}$, for $i = 1, \ldots, n$. The goal of subspace clustering is to segment the columns of X into their corresponding subspaces.*

In the past decade, subspace clustering has become an important topic in unsupervised learning and many subspace clustering algorithms have been developed [2, 21, 4, 25, 20, 24, 5, 17, 34, 48, 18]. These methods have been successfully applied to various applications such as motion segmentation [42, 38], face image clustering [3], genes expression array clustering [26] and so on.

Despite the great success in the recent development of subspace clustering, its applicability to real applications is very limited because practical data do not necessarily conform with the linear subspace model. In face image clustering, for example, practical face images are often not aligned and often contain variations in pose and expression of the subject. Subspace clustering cannot handle such cases as images corresponding to the same face no longer lie in linear subspaces. While there are recently developed techniques for jointly image alignment and subspace clustering [19], such a parameterized model is incapable of handling a broader range of data variations such as deformation, translation and so on. It is also possible to use manually designed invariance features such as SIFT [23], HOG [1] and PRICoLBP [36] of the images before performing subspace clustering. However, there has been neither theoretical nor practical evidence to show that such features follow the linear subspace model.

Recently, convolutional neural networks (ConvNets) have demonstrated superior ability in learning useful image representations in a wide range of tasks such as face/object classification and detection [15, 28]. In particular, it is

shown in [16] that when applied to images of different classes, ConvNets are able to learn features that lie in a union of linear subspaces. The challenge for training such a ConvNet, however, is that it requires a large number of labeled training images which is often unavailable in practical applications.

In order to train ConvNet for feature learning without labeled data, many methods have been recently proposed by exploiting the self-expression of data in a union of subspaces [33, 12, 32, 50]. Specifically, these methods supervise the training of ConvNet by inducing the learned features to be such that each feature vector can be expressed as a linear combination of the other feature vectors. However, it is difficult to learn good feature representations in such an approach due to the lack of effective supervision.

Paper contribution. In this paper, we develop an end-to-end trainable framework for simultaneously feature learning and subspace clustering, called Self-Supervised Convolutional Subspace Clustering Network (S^{2}ConvSCN). In this framework, we use the current clustering results to self-supervise the training of feature learning and self-expression modules, which is able to significantly improve the subspace clustering performance. In particular, we introduce the following two self-supervision modules:

1. We introduce a spectral clustering module which uses the current clustering results to supervise the learning of the self-expression coefficients. This is achieved by inducing the affinity generated from the self-expression to form a segmentation of the data that aligns with the current class labels generated from clustering.

2. We introduce a classification module which uses the current clustering results to supervise the training of feature learning. This is achieved by minimizing the classification loss between the output of a classifier trained on top of the feature learning module and the current class labels generated from clustering.

We propose a training framework where the feature representation, the data self-expression and the data segmentation are jointly learned and alternately refined in the learning procedure. Conceptually, the initial clustering results do not align exactly with the true data segmentation, therefore the initial self-supervision incurs errors to the training. Nonetheless, the feature learning is still expected to benefit from such self-supervision as there are data with correct labels that produce useful information. An improved feature representation subsequently helps to learn a better self-expression and consequently produce a better data segmentation (i.e., with less wrong labels). Our experiments on four benchmark datasets demonstrate superior performance of the proposed approach.

2. Related Work

In this section, we review the relevant prior work in subspace clustering. For clarity, we group them into two categories: a) subspace clustering in original space; and b) subspace clustering in feature space.

2.1. Subspace Clustering in Original Space

In the past years, subspace clustering has received a lot of attention and many methods have been developed. Among them, methods based on spectral clustering are the most popular, e.g., [2, 21, 4, 25, 3, 20, 24, 5, 17, 34, 48, 18, 47]. These methods divide the task of subspace clustering into two subproblems. The first subproblem is to learn a data affinity matrix from the original data, and the second subproblem is to apply spectral clustering on the affinity matrix to find the segmentation of the data. The two subproblems are solved successively in one-pass [2, 21, 4, 25, 24, 48] or solved alternately in multi-pass [5, 17, 18].

Finding an informative affinity matrix is the most crucial step. Typical methods to find an informative affinity matrix are based on the self-expressiveness property of data [2], which states that a data point in a union of subspaces can be expressed as a linear combination of other data points, i.e., $\mathbf{x}_j = \sum_{i \neq j} c_{ij}\mathbf{x}_i + \mathbf{e}_j$, where $\mathbf{e}_j$ is used to model the noise or corruption in data. It is expected that the linear combination of data point $\mathbf{x}_j$ uses the data points that belong to the same subspace as $\mathbf{x}_j$. To achieve this objective, different types of regularization terms on the linear combination coefficients are used. For example, in [2] the ℓ_1 norm is used to find sparse linear combination; in [21] the nuclear norm of the coefficients matrix is used to find low-rank representation; in [43, 48] the mixture of the ℓ_1 norm and the ℓ_2 norm or the nuclear norm is used to balance the sparsity and the denseness of the linear combination coefficients; and in [45] a data-dependent sparsity-inducing regularizer is used to find sparse linear combination. On the other hand, different ways to model the noise or corruptions in data have also been investigated, e.g., the vector ℓ_1 norm is used in [2], the $\ell_{2,1}$ norm is adopted in [21], and the correntropy term is used in [8].

2.2. Subspace Clustering in Feature Space

For subspace clustering in feature space, we further divide the ways to form the feature space into two types: a) *Latent feature space*, which is induced via a Mercer kernel, e.g., [31, 29, 46, 44], or constructed via matrix decomposition, e.g., [22], [30]; b) *Explicit feature space*, which is designed by manually feature extraction, e.g., [33], or learnt from data, e.g., [12, 50].

Latent Feature Space. Standard subspace clustering methods handle data point lie in a union of linear (or affine) subspaces in the original data space, which assume that

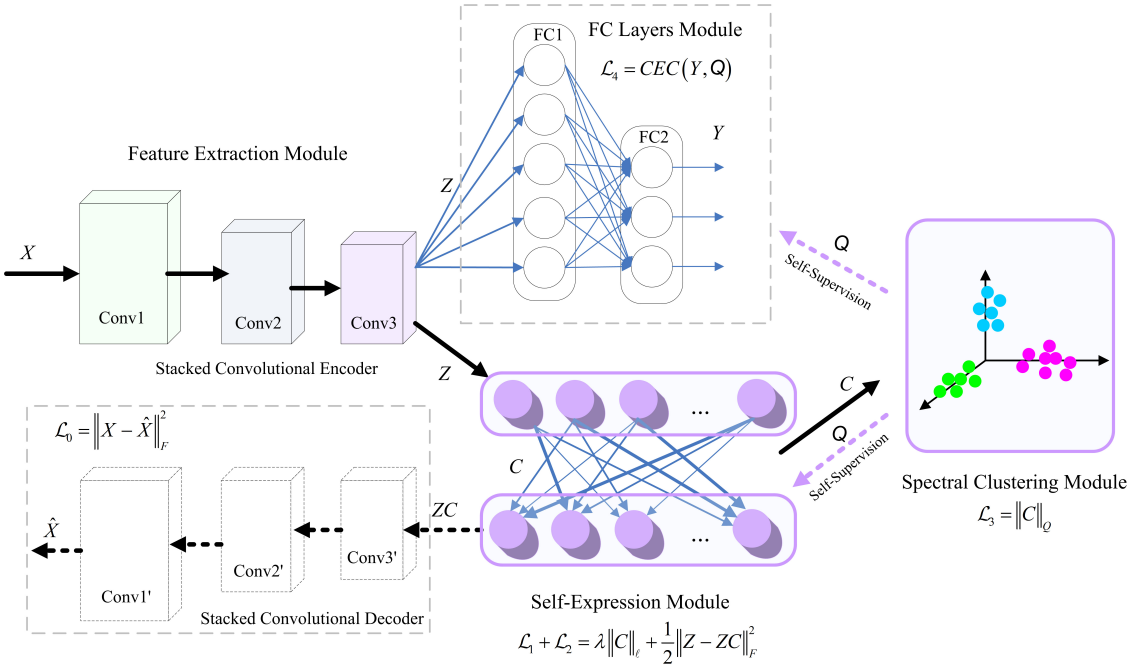

Figure 1. Architecture of the proposed Self-Supervised Convolutional Subspace Clustering Network (S^{2}ConvSCN). It consists of mainly five modules: a) stacked convolutional encoder module, which is used to extract convolutional features; b) stacked convolutional decoder module, which is used with the encoder module to initialize the convolutional module; c) self-expression module, which is used to learn the self-expressive coefficient matrix and also takes the self-supervision information from the result of spectral clustering to refine the self-expressive coefficients matrix; d) FC-layers based self-supervision module, which builds a self-supervision path back to the stacked convolutional encoder module; e) spectral clustering module, which provides self-supervision information to guide the self-expressive model and FC-layers module. The modules with solid line box are the backbone components; whereas the modules in dashed box are the auxiliary components to facilitate the training of the whole network.

each sample can be linearly reconstructed by the rest sample. However, in the realworld applications, the original data may not be linearly represented by other points in the datasets.

To address this problem, kernel trick is employed to yield a latent feature space implicitly where subspace clustering is conducted accordingly, e.g., [31, 29, 46, 44]. In [31, 29], kernel sparse subspace clustering (KSSC) is proposed, in which the predefined polynomial kernel and Gaussian kernel are investigated. In [46, 44], similarly, kernel low-rank representation (KLRR) is presented. While it seems appealing to map the original data into high dimensional feature space via a nonlinear kernel implicitly, how to select a kernel function to suite for the original data well is still an open issue.

On the other hand, the latent feature space can also be constructed via matrix decomposition, e.g., [22], [30]. In [22], linear transform matrix and low-rank representation are computed simultaneously; in [30], linear transform matrix and sparse representation are jointly optimized. However, why and how the learned linear transform could bring performance improvement are still unclear.

Explicit Feature Space. In recent years, deep learning has increasingly gained a lot of research interests due to its powerful ability to learn hierarchical features in an end-to-end trainable way [9, 14], [35]. Recently, there are a few attempts to borrow deep learning framework to conduct feature extraction for subspace clustering. For example, a fully connected deep auto-encoder network with handcrafted features (e.g., SIFT or HOG features) combined with a sparse self-expressive model is developed in [33]; a stacked convolutional auto-encoder network with a plus-in self-expressive model is proposed in [12]; a deep adversarial network with a subspace-specific generator and a discriminator is presented in [50]. While promising clustering accuracy has been shown, these methods are still suboptimal because *neither* the potentially useful supervision information from the clustering result has been taken into the feature learning step *nor* a joint optimization framework for fully combining feature learning and subspace clustering has been developed.

In this paper, we attempt to develop a joint optimization framework for combining feature learning and subspace clustering, such that the useful self-supervision information from subspace clustering result could be used to guide the feature learning step and to refine the self-expressiveness model. Inspired by the success of Convolutional Neural Networks in recent years for classification tasks on images

and videos datasets [14], we integrate the convolutional feature extraction module into subspace clustering to form an end-to-end trainable joint optimization framework, called Self-Supervised Convolutional Subspace Clustering Network (S^{2}ConvSCN). In S^{2}ConvSCN, both the stacked convolutional layers based feature extraction and the self-expressiveness based affinity learning are effectively self-supervised by exploiting the feedback from spectral clustering. We design two-stage procedure based approach to train the proposed framework and conduct extensive experiments on benchmark datasets. Experimental results demonstrate superior performance of our proposal.

3. Our Proposal: Self-Supervised Convolutional Subspace Clustering Network

In this section, we present our S^{2}ConvSCN for joint feature learning and subspace clustering. We start with introducing our network formulation (see Fig. 1), then introduce the self-supervision modules. Finally, we present an effective algorithm for training the proposed network.

3.1. Network Formulation

As aforementioned, our network is composed of a feature extraction module, a self-expression module and self-supervision modules for training the former two modules.

Feature Extraction Module. A basic component of our proposed S^{2}ConvSCN is the feature extraction module, which is used to extract features from raw data that are amenable to subspace clustering. To extract localized features while preserving spatial locality, we adopt the convolutional neural network which is comprised of multiple convolutional layers. We denote the input to the network as $\mathbf{h}^{(0)} = \mathbf{x}$ where $\mathbf{x}$ is the image. A convolutional layer ℓ contains a set of filters $\mathbf{w}_i^{(\ell)}$ and the associated biases $\mathbf{b}_i^{(\ell)}$, $i = 1, \cdots, m^{(\ell)}$, and produces $m^{(\ell)}$ feature maps from the output of the previous layer as

$$\mathbf{h}_i^{(\ell)} = \sigma(\mathbf{h}^{(\ell-1)} * \mathbf{w}_i^{(\ell)} + \mathbf{b}_i^{(\ell)}), i = 1, \cdots, m^{(\ell)} \quad (1)$$

where $\sigma(\cdot)$ is an activation function and $*$ denotes the convolution. The feature maps $\{\mathbf{h}_i^{(L)}\}_{i=1,\cdots,m^{(L)}}$ in the top layer L of the network are then used to form a representation of the input data $\mathbf{x}$. Specifically, the $m^{(L)}$ feature maps $\{\mathbf{h}_i^{(L)}\}_{i=1}^{m^{(L)}}$ are vectorized and concatenated to form a representation vector $\mathbf{z}$, i.e.,

$$\mathbf{z} = \left[\mathbf{h}_1^{(L)}(:), \cdots, \mathbf{h}_{m^{(L)}}^{(L)}(:)\right]^\top, \quad (2)$$

where $\mathbf{h}_1^{(L)}(:), \cdots, \mathbf{h}_{m^{(L)}}^{(L)}(:)$ are row vectors denoting the vectorization of the feature maps $\mathbf{h}_1^{(L)}, \cdots, \mathbf{h}_{m^{(L)}}^{(L)}$. These vectors are horizontally concatenated and then transposed to form the vector $\mathbf{z}$.

To ensure that the learned representation $\mathbf{z}$ contains meaningful information from the input data $\mathbf{x}$, such representation is fed into a decoder network to reconstruct an image $\hat{\mathbf{x}}$. The loss function for this encoder-decoder network is the reconstruction error:

$$\mathcal{L}_0 = \frac{1}{2N}\sum_{j=1}^{N}\|\mathbf{x}_j - \hat{\mathbf{x}}_j\|_2^2 = \frac{1}{2N}\|X - \hat{X}\|_F^2, \quad (3)$$

where N is the number of images in the training set.

Self-Expression Module. State-of-the-art subspace clustering methods are based on the self-expressiveness property of data, which states that each data point in a union of subspaces can be expressed as a linear combination of other data points [3]. In order to learn feature representations that are suitable for subspace clustering, we adopt a self-expression module that imposes the following loss function:

$$\lambda_1\|C\|_\ell + \frac{\lambda_2}{2}\|Z - ZC\|_F^2 \text{ s.t. } \text{diag}(C) = \mathbf{0}, \quad (4)$$

where $Z = \left[\mathbf{z}_1, \cdots, \mathbf{z}_N\right]$ is a matrix containing features from the feature extraction module as its columns, $\|C\|_\ell$ is a properly chosen regularization term, the constraint $\text{diag}(C) = \mathbf{0}$ is optionally used to rule out a trivial solution of $C = I$, and $\lambda_1 > 0$, $\lambda_2 > 0$ are tradeoff parameters.

Self-Supervision Modules. Once the self-expression coefficient matrix C is obtained, we can compute a data affinity matrix as $A = \frac{1}{2}(|C| + |C^\top|)$. Subsequently, spectral clustering can be applied which obtains a segmentation of the data by minimizing the following cost:

$$\min_{Q} \sum_{i,j} a_{ij}\|\mathbf{q}_i - \mathbf{q}_j\|_2^2, \text{ s.t. } Q \in \mathcal{Q}, \quad (5)$$

where $\mathcal{Q} = \{Q \in \{0,1\}^{n\times N} : \mathbf{1}^\top Q = \mathbf{1}^\top \text{ and } \text{rank}(Q) = n\}$ is a set of all valid segmentation matrices, and $\mathbf{q}_i$ and $\mathbf{q}_j$ are respectively the i-th and j-th columns of Q indicating the membership of each data point to the assigned cluster. In practice, since the search over all $Q \in \mathcal{Q}$ is combinatorial, spectral clustering techniques usually relax the constraint $Q \in \mathcal{Q}$ to $QQ^\top = I$.

Observe that the spectral clustering produces a labeling of the data set which, albeit is not necessarily the correct class label for all the data points, contains meaningful information about the data. This motivates us to supervise the training of the feature extraction and self-expression modules using the output of spectral clustering. In principle, the features learned from the feature extraction module should contain enough information for predicting the class labels of the data points. Therefore, we introduce a classification layer on top of the feature extraction module which is expected to produce labels that aligns with the labels generated in spectral clustering. Furthermore, the segmentation produced by spectral clustering can also be used to construct a

binary segmentation matrix, which contains information regarding which data points should be used in the expression of a particular data points. Therefore, we incorporate the objective function of spectral clustering as a loss function in our network formulation, which has the effect of supervising the training of the self-expression module. We present the details of these two self-supervision modules in the following two subsections.

3.2. Self-Supervision for Self-Expression

To exploit the information in the labels produced by spectral clustering, we incorporate spectral clustering as a module of the network which provides a feedback to the self-expression model (see Fig. 1).

To see how the spectral clustering objective function in (5) provides such feedback, note that (5) can be rewritten as a weighted ℓ_1 norm of C [17], that is,

$$\frac{1}{2}\sum_{i,j} a_{ij}\|\mathbf{q}_i - \mathbf{q}_j\|_2^2 = \sum_{i,j}|c_{ij}|\frac{\|\mathbf{q}_i - \mathbf{q}_j\|_2^2}{2} := \|C\|_Q, \quad (6)$$

where we have used the fact that $a_{ij} = \frac{1}{2}(|c_{ij}| + |c_{ji}|)$. It can be seen from (6) that $\|C\|_Q$ measures the discrepancy between the coefficients matrix C and the segmentation matrix Q. When Q is provided, minimizing the cost $\|C\|_Q$ has the effect of enforcing the self-expression matrix C to be such that an entry c_{ij} is nonzero only if the i-th and j-th data points have the same class labels. Therefore, incorporating the term $\|C\|_Q$ in the network formulation helps the training of the self-expression module. That is, the result of previous spectral clustering can be incorporated into the self-expressive model to provide self-supervision for refining the self-expression matrix C.

3.3. Self-Supervision for Feature Learning

We also use the class labels generated from spectral clustering to supervise the training of the feature extraction module. Notice that the output of spectral clustering is an n-dimensional vector which indicates the membership to n subspaces (i.e., clusters). Thus, we design FC layers as $p \times N_1 \times N_2 \times n$, where p is the dimension of the extracted convolutional feature, which is defined as the concatenation of the different feature maps of the last convolutional layer in the encoder block, and N_1 and N_2 are the numbers of neurons in the two FC layers, respectively.

Denote $\mathbf{y}$ as the n-dimensional output of the FC layers, where $\mathbf{y} \in I\!R^n$. Note that the output $\{\mathbf{q}_j\}_{j=1}^N$ of spectral clustering will be treated as the target output of the FC layers. To exploit the self-supervision information to train the convolutional encoder, we define a mixture of *cross-entropy loss* and *center loss* (CEC) as follows:

$$\mathcal{L}_4 = \frac{1}{N}\sum_{j=1}^{N}(\ln(1 + \mathrm{e}^{-\tilde{\mathbf{y}}_j^\top \mathbf{q}_j}) + \tau\|\mathbf{y}_j - \mu_{\pi(\mathbf{y}_j)}\|_2^2), \quad (7)$$

where $\tilde{\mathbf{y}}_j$ is a normalization of $\mathbf{y}_j$ via *softmax*, $\mu_{\pi(\mathbf{y}_j)}$ denotes the cluster center which corresponds to $\mathbf{y}_j$, $\pi(\mathbf{y}_j)$ is to take the index of $\mathbf{y}_j$ from the output of spectral clustering, and $0 \leq \tau \leq 1$ is a tradeoff parameter. The first term of $\mathcal{L}_4$ is effectively a cross-entropy loss and the second term of $\mathcal{L}_4$ is a center loss which compresses the intra-cluster variations.

An important issue in defining such a loss function is that the output of spectral clustering $\{\mathbf{q}_j\}_{j=1}^N$ provides merely *pseudo labels* for the input data. That is, specific label index assigned to each cluster is up to a permutation. Therefore, the class labels from two successive iterations might not be consistent. To address this issue, we perform a permutation of the pseudo labels so that it is most consistent with pseudo labels from the previous iteration before feeding into the self-supervision module with the cross-entropy part as in (7).

Remark 1. Note that the output of spectral clustering is used in two interrelated self-supervision modules. Thus, we call it a dual self-supervision. Owing to effectively exploiting the self-supervision information, our proposed S^{2}ConvSCN yields superior performance.

3.4. Training S^{2}ConvSCN

We design the total cost function by putting together the costs of the five components (i.e., $\mathcal{L}_0$, $\mathcal{L}_1$, $\mathcal{L}_2$, $\mathcal{L}_3$ and $\mathcal{L}_4$) as following:

$$\mathcal{L} = \mathcal{L}_0 + \gamma_1\mathcal{L}_1 + \gamma_2\mathcal{L}_2 + \gamma_3\mathcal{L}_3 + \gamma_4\mathcal{L}_4, \quad (8)$$

where $\mathcal{L}_0$ is defined in (3), $\mathcal{L}_1 = \|C\|_\ell$, $\mathcal{L}_2 = \frac{1}{2}\|Z - ZC\|_F^2$, $\mathcal{L}_3 = \|C\|_Q$, $\mathcal{L}_4$ is defined in (7), and γ_1, γ_2, γ_3 and γ_4 are four tradeoff parameters. The tradeoff parameters are set to be roughly inversely proportional to the value of each cost in order to obtain a balance amongst them.

To train S^{2}ConvSCN, we propose a two-stage strategy as follows: a) Pre-train the stacked convolutional layers to provide an initialization of S^{2}ConvSCN; b) Train the whole network with the assistance of the self-supervision information provided by spectral clustering.

Stage I: Pre-Training Stacked Convolutional Module. The pre-training stage uses the cost $\mathcal{L}_0$. In this stage, we set the weights in the two FC layers as zeros, which yield zeros output. Meanwhile, we also set the output of spectral clustering as zero vectors, i.e., $\mathbf{q}_j = 0$ for $j = 1, \cdots, N$. By doing so, the two FC layers are "sleeping" during this pre-training stage. Moreover, we set the coefficient matrix C as an identity matrix, which is equivalent to training S^{2}ConvSCN without the self-expressive layer.

Algorithm 1 Procedure for training S^{2}ConvSCN

Require: Input data, tradeoff parameters, maximum iteration T_{max}, T_0, and t=1.

1. Pre-train the stacked convolutional module via stacked CAE.
2. (Optional) Pre-train the stacked convolutional module with the self-expressive layer.
3. Initialize the FC layers.
4. Run self-expressive layer.
5. Run spectral clustering layer to get the segmentation Q.
6. **while** $t \leq T_{max}$ **do**
   Fixed Q, update the other parts T_0 epoches.
   Run spectral clustering once to update Q and set $t \leftarrow t+1$.
7. **end while**

Ensure: trained S^{2}ConvSCN and Q.

As an optional pre-training, we can also use the pre-trained stacked CAE to train the stacked CAE with the self-expressive layer. This is in fact a DSCNet, which is investigated in [12].

Stage II: Training the Whole S^{2}ConvSCN. In this stage, we use the total cost $\mathcal{L}$ to train the whole S^{2}ConvSCN as a stacked CAE assisted with the self-expressiveness module and dual self-supervision. To be more specific, given the spectral clustering result Q, we update the other parameters in S^{2}ConvSCN for T_0 epoches, and then we perform spectral clustering to update Q. For clarity, we provide the detailed procedure to train S^{2}ConvSCN in Algorithm 1.

Remark 2. In the total cost function as (8), if we set $\gamma_3 = \gamma_4 = 0$, then the two self-supervision blocks will disappear and our S^{2}ConvSCN reduces to DSCNet [12]. Thus, it would be interesting to add an extra pre-training stage, i.e., using the cost function $\mathcal{L}_0 + \gamma_1\mathcal{L}_1 + \gamma_2\mathcal{L}_2$ to train the stacked convolutional module and the self-expressive layer together before evoking the FC layers and the spectral clustering layer. This is effectively a DSCNet [12]. In experiments, as used in [12], we stop the training by setting a maximum number of epoches $T_{\max}$.

4. Experimental Evaluations

To evaluate the performance of our proposed S^{2}ConvSCN, we conduct experiments on four benchmark data sets: two face image data sets, the Extended Yale B [6] and ORL [37], and two object image data sets, COIL20 and COIL100 [27]. We compare our proposed S^{2}ConvSCN with nine baseline algorithms, including Low Rank Representation (LRR) [21], Low Rank Subspace Clustering (LRSC) [41], Sparse Subspace Clustering (SSC) [3], Kernel Sparse Subspace Clustering (KSSC) [31], SSC by Orthogonal Matching Pursuit (SSC-OMP) [49], Efficient Dense Subspace Clustering (EDSC) [11], SSC with the pre-trained convolutional auto-encoder features (AE+SSC), EDSC with the pre-trained convolutional auto-encoder features (AE+EDSC), and Deep Subspace Clustering Networks (DSCNet) [12]. For AE+SSC, AE+EDSC, and DSCNet, we directly cite the best results reported in [12].

	Extended Yale B		ORL	
Layers	kernel size	channels	kernel size	channels
encoder-1	5×5	10	3×3	3
encoder-2	3×3	20	3×3	3
encoder-3	3×3	30	3×3	5
decoder-1	3×3	30	3×3	5
decoder-2	3×3	20	3×3	3
decoder-3	5×5	10	3×3	3

Table 1. Network settings for Extended Yale B and ORL.

The architecture specification of S^{2}ConvSCN used in our experiments for each dataset are listed in Table 1 and Table 4. In the stacked convolutional layers, we set the kernel stride as 2 in both horizontal and vertical directions, and use Rectified Linear Unit (ReLU) [14] as the activation function $\sigma(\cdot)$. In addition, the learning rate is set to 1.0×10^{-3} in all our experiments. The whole data set is used as one batch input. For the FC layers, we set $N_1 = \frac{N}{2}$ and $N_2 = n$.

To find informative affinity matrix, we adopt the vector ℓ_1 norm and the vector ℓ_2 norm to define $\|C\|_\ell$ and denote them as S^{2}ConvSCN-ℓ_1 and S^{2}ConvSCN-ℓ_2, respectively. In the second training stage, we update the stacked convolutional layers, the self-expressive model, and the FC layers for T_0 epochs and then update the spectral clustering module once, where T_0 is set to $5 \sim 16$ in our experiments.

4.1. Experiments on Extended Yale B

The Extended Yale B Database [6] consists of face images of 38 subjects, 2432 images in total, with approximately 64 frontal face images per subject taken under different illumination conditions, where the face images of each subject correspond to a low-dimensional subspace. In our experiments, we follow the protocol used in [12]: a) each image is down-sampled from 192×168 to 48×42 pixels; b) experiments are conducted using all choices of $n \in \{10, 15, 20, 25, 30, 35, 38\}$.

To make a fair comparison, we use the same setting as that used in DSCNet [12], in which a three-layer stacked convolutional encoders is used with $\{10, 20, 30\}$ channels, respectively. The detailed settings for the stacked convolutional network used on Extended Yale B are shown Table 1. The common regularization parameters γ_1 and γ_2 are set

Methods	LRR	LRSC	SSC	AE+ SSC	KSSC	SSC-OMP	EDSC	AE+ EDSC	DSCNet-ℓ_1	DSCNet-ℓ_2	S^{2}ConvSCN-ℓ_2	S^{2}ConvSCN-ℓ_1
10 subjects												
Mean	22.22	30.95	10.22	17.06	14.49	12.08	5.64	5.46	2.23	1.59	**1.18**	**1.18**
Median	23.49	29.38	11.09	17.75	15.78	8.28	5.47	6.09	2.03	1.25	**1.09**	**1.09**
15 subjects												
Mean	23.22	31.47	13.13	18.65	16.22	14.05	7.63	6.70	2.17	1.69	1.14	**1.12**
Median	23.49	31.64	13.40	17.76	17.34	14.69	6.41	5.52	2.03	1.72	**1.14**	**1.14**
20 subjects												
Mean	30.23	28.76	19.75	18.23	16.55	15.16	9.30	7.67	2.17	1.73	1.31	**1.30**
Median	29.30	28.91	21.17	16.80	17.34	15.23	10.31	6.56	2.11	1.80	1.32	**1.25**
25 subjects												
Mean	27.92	27.81	26.22	18.72	18.56	18.89	10.67	10.27	2.53	1.75	1.32	**1.29**
Median	28.13	26.81	26.66	17.88	18.03	18.53	10.84	10.22	2.19	1.81	1.34	**1.28**
30 subjects												
Mean	37.98	30.64	28.76	19.99	20.49	20.75	11.24	11.56	2.63	2.07	1.71	**1.67**
Median	36.82	30.31	28.59	20.00	20.94	20.52	11.09	10.36	2.81	2.19	1.77	**1.72**
35 subjects												
Mean	41.85	31.35	28.55	22.13	26.07	20.29	13.10	13.28	3.09	2.65	1.67	**1.62**
Median	41.81	31.74	29.04	21.74	25.92	20.18	13.10	13.21	3.10	2.64	1.69	**1.60**
38 subjects												
Mean	34.87	29.89	27.51	25.33	27.75	24.71	11.64	12.66	3.33	**2.67**	1.56	**1.52**
Median	34.87	29.89	27.51	25.33	27.75	24.71	11.64	12.66	3.33	**2.67**	1.56	**1.52**

Table 2. Clustering Error (%) on Extended Yale B. The best results are in bold and the second best results are underlined.

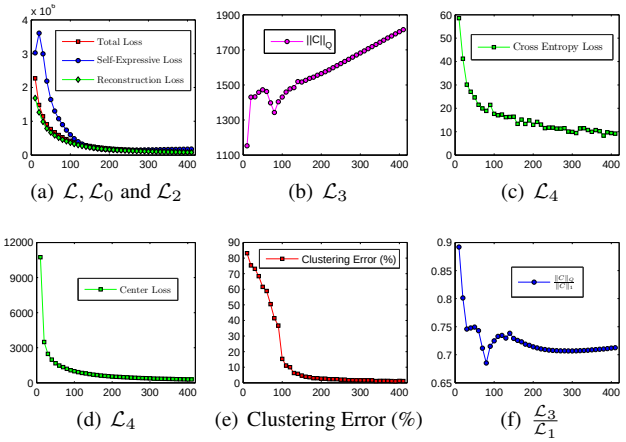

(a) $\mathcal{L}$, $\mathcal{L}_0$ and $\mathcal{L}_2$ (b) $\mathcal{L}_3$ (c) $\mathcal{L}_4$

(d) $\mathcal{L}_4$ (e) Clustering Error (%) (f) $\frac{\mathcal{L}_3}{\mathcal{L}_1}$

Figure 2. The cost functions and clustering error of S^{2}ConvSCN-ℓ_1 during training period on Extended Yale B ($n = 10$).

the same as that in DSCNet, where $\gamma_1 = 1$ (for the term $\|C\|_\ell$) and $\gamma_2 = 1.0 \times 10^{\frac{n}{10}-3}$. For the specific parameters used in S^{2}ConvSCN, we set $\gamma_3 = 16$ for the term $\|C\|_Q$ and $\gamma_4 = 72$ for the cross-entropy term, respectively. We set $T_0 = 5$, set $T_{\max}$ to $10 + 40n$, where n is the number of clusters.

The experimental results are presented in Table 2. We observe that our proposed S^{2}ConvSCN-ℓ_1 and S^{2}ConvSCN-ℓ_2 remarkably reduced the clustering errors and yield the lowest clustering errors with $n \in \{10, 15, 20, 25, 30, 35, 38\}$ than all the listed baseline methods.

To gain further understanding of the proposed dual self-supervision, we use S^{2}ConvSCN-ℓ_1 as an example and evaluate the effect of using the dual self-supervision modules via an ablation study. Due to space limitation, we only list the experimental results of using a single self-supervision via $\mathcal{L}_3$, using a single self-supervision via $\mathcal{L}_4$, and using dual self-supervision of $\mathcal{L}_3$ plus $\mathcal{L}_4$ on datasets Extended Yale B in Table 3. As a baseline, we show the experimental results of DSCNet [13], which uses the loss $\mathcal{L}_0 + \mathcal{L}_1 + \mathcal{L}_2$. As could be read from Table 3 that, using only a single self-supervision module, i.e., $\mathcal{L}_0 + \mathcal{L}_1 + \mathcal{L}_2$ plus $\mathcal{L}_3$, or $\mathcal{L}_0 + \mathcal{L}_1 + \mathcal{L}_2$ plus $\mathcal{L}_4$, the clustering error could be reduced. Compared to using the self-supervision via a spectral clustering loss $\mathcal{L}_3$ in the self-expression module, using the self-supervision via the classification loss $\mathcal{L}_4$ in FC block is more effective. Nonetheless, using the dual supervision modules further reduce the clustering errors.

4.2. Experiments on ORL

The ORL data set [37] consists of face images of 40 distinct subjects, each subjects having 10 face images under varying lighting conditions, with different facial expressions (open/closed eyes, smiling/not smiling) and facial details (glasses / no glasses) [37]. As the images were took under variations of facial expressions, this data set is more challenging for subspace clustering due to the nonlinearity and small sample size per subject.

In our experiments, each image is down-sampled from 112×92 to 32×32. We reduce the kernel size in convolution module to 3×3 due to small image size and set the number of channels to $\{3, 3, 5\}$. The specification of the network structure is shown in Table 1. For the tradeoff parameters, we set $\gamma_1 = 0.1, \gamma_2 = 0.01, \gamma_3 = 8$, and $\gamma_4 = 1.2$ for our S^{2}ConvSCN. For the fine-tuning stage, we set $T_0 = 5$ and the number of maximum epochs $T_{\max} = 940$.

Experimental results are shown in Table 5. Again, our proposed approaches yield the best results.

4.3. Experiments on COIL20 and COIL100

To further verify the effectiveness of our proposed S^{2}ConvSCN, we conduct experiments on data set COIL20 and COIL100 [27]. COIL20 contains 1440 gray-scale images of 20 objects; whereas COIL100 contains 7200 images of 100 objects. Each image was down-sampled to 32×32.

Losses \ No. Subjects	10 subjects		15 subjects		20 subjects		25 subjects		30 subjects		35 subjects		38 subjects	
	Mean	Median	Mean	Median	Mean	Median	Mean	Median	Mean	Median	Mean	Median	Mean	Median
$\mathcal{L}_0+\mathcal{L}_1+\mathcal{L}_2$(DSC [12])	2.23	2.03	2.17	2.03	2.17	2.11	2.53	2.19	2.63	2.81	3.09	3.10	3.33	3.33
$\mathcal{L}_0+\mathcal{L}_1+\mathcal{L}_2+\mathcal{L}_3$	1.58	1.25	1.63	1.55	1.67	1.57	1.61	1.63	2.74	1.82	2.64	2.65	2.75	2.75
$\mathcal{L}_0+\mathcal{L}_1+\mathcal{L}_2+\mathcal{L}_4$	1.32	**1.09**	1.31	1.30	1.54	1.48	1.48	1.98	1.87	**1.61**	1.82	1.84	1.92	1.92
$\mathcal{L}_0+\mathcal{L}_1+\mathcal{L}_2+\mathcal{L}_3+\mathcal{L}_4$	**1.18**	**1.09**	**1.12**	**1.14**	**1.30**	**1.25**	**1.29**	**1.28**	**1.67**	1.72	**1.62**	**1.60**	**1.52**	**1.52**

Table 3. Ablation Study on S^{2}ConvSCN-ℓ_1 on Extended Yale B.

	COIL20		COIL100	
Layers	kernel size	channels	kernel size	channels
encoder-1	3×3	15	5×5	50
decoder-1	3×3	15	5×5	50

Table 4. Network settings for COIL20 and COIL100.

The settings of the stacked convolutional networks used for COIL20 and COIL100 are listed in Table 4.

For the tradeoff parameters on COIL20, we set $\gamma_1=1$, $\gamma_2=30$ as same as used in DSC-Net [12], and $\gamma_3=8$, $\gamma_4=6$, $T_0=4$, and $T_{\max}=80$ in our S^{2}ConvSCN. For the tradeoff parameters on COIL100, we set $\gamma_1=1$, $\gamma_2=30$ as same as used in DSC-Net [12], and $\gamma_3=8$, $\gamma_4=7$, $T_0=16$, and $T_{\max}=110$ in our S^{2}ConvSCN.

For experiments on COIL20 and COIL100, we initialize the convolutional module with stacked CAE at first, and then train a stacked CAE assisted with a self-expressive model. This is effectively DSCNet [12]. And then, we train the whole S^{2}ConvSCN. Experimental results are listed in Table 5. As could be read, our S^{2}ConvSCN-ℓ_1 and S^{2}ConvSCN-ℓ_2 reduce the clustering errors significantly. This result confirms the effectiveness of the designed dual self-supervision components for the proper use of the useful information from the output of spectral clustering.

4.4. Convergence Behaviors

To show the convergence behavior during training iterations, we conduct experiments on Extended Yale B with $n=10$. We record the clustering errors and each cost function during training period, and show them as a function of the number of epoches in Fig. 2. As could be observed from Fig. 2(a), (c), (d) and (e), the cost functions $\mathcal{L}$, $\mathcal{L}_0$, $\mathcal{L}_2$, and $\mathcal{L}_4$, and the cluster error decrease rapidly and tend to "flat". To show more details in the iterations, in Fig. 2 (b) and (f), we show the curve of $\|C\|_Q$ and $\frac{\|C\|_Q}{\|C\|_1}$. Note that $\|C\|_Q$ and $\frac{\|C\|_Q}{\|C\|_1}$ are the cost and the relative cost of spectral clustering, respectively. Compared to $\|C\|_Q$, we argue that $\frac{\|C\|_Q}{\|C\|_1}$ is more indicative to the clustering performance. As could be observed, while $\|C\|_Q$ is increasing, the curve of $\frac{\|C\|_Q}{\|C\|_1}$ tends to "flat"—which is consistent to the curve of the clustering error.

Methods	ORL	COIL20	COIL100
LRR	38.25	31.01	59.82
LRSC	32.50	31.25	50.67
SSC	32.50	14.86	45.00
AE+SSC	26.75	22.08	43.93
KSSC	34.25	24.65	47.18
SSC-OMP	36.00	45.90	66.39
EDSC	27.25	14.86	38.13
AE+EDSC	26.25	14.79	38.88
DSC-ℓ_2	14.00	5.42	30.96
DSC-ℓ_1	14.25	5.65	33.62
S^{2}ConvSCN-ℓ_2	11.25	2.33	27.83
S^{2}ConvSCN-ℓ_1	**10.50**	**2.14**	**26.67**

Table 5. Clustering Error (%) on ORL, COIL20 and COIL100.

5. Conclusion

We have proposed an end-to-end trainable framework for simultaneously feature learning and subspace clustering, called Self-Supervised Convolutional Subspace Clustering Network (S^{2}ConvSCN). More specifically, in S^{2}ConvSCN, the hierarchical feature extraction via stacked convolutional module, the affinity learning via self-expressiveness model, and the data segmentation via spectral clustering are integrated into a joint optimization framework. By exploiting a dual self-supervision, the output of spectral clustering are effectively used to improve the training of the stacked convolutional module and to refine the self-expressiveness model, leading to superior performance. Experiments conducted on benchmark data sets have validated the effectiveness of our proposed approach.

References

[1] N. Dalal and B. Triggs. Histograms of oriented gradients for human detection. In *IEEE Conference on Computer Vision and Pattern Recognition*, 2005. 1

[2] E. Elhamifar and R. Vidal. Sparse subspace clustering. In *Proceedings of IEEE International Conference on Computer Vision and Pattern Recognition*, pages 2790–2797, 2009. 1, 2

[3] E. Elhamifar and R. Vidal. Sparse subspace clustering: Algorithm, theory, and applications. *IEEE Transactions on Pattern Analysis and Machine Intelligence*, 35(11):2765–2781, 2013. 1, 2, 4, 6

[4] P. Favaro, R. Vidal, and A. Ravichandran. A closed form solution to robust subspace estimation and clustering. In *IEEE Conference on Computer Vision and Pattern Recognition*, pages 1801 –1807, 2011. 1, 2

[5] J. Feng, Z. Lin, H. Xu, and S. Yan. Robust subspace segmentation with block-diagonal prior. In *IEEE Conference on Computer Vision and Pattern Recognition*, pages 3818–3825, 2014. 1, 2

[6] A.-S. Georghiades, P.-N. Belhumeur, and D.-J. Kriegman. From few to many: Illumination cone models for face recognition under variable lighting and pose. *IEEE Transactions on Pattern Analysis and Machine Intelligence*, 23(6):643–660, 2001. 6

[7] T. Hastie and P.-Y. Simard. Metrics and models for handwritten character recognition. *Statistical Science*, pages 54–65, 1998. 1

[8] R. He, L. Wang, Z. Sun, Y. Zhang, and B. Li. Information theoretic subspace clustering. *IEEE Transactions on Neural Networks and Learning Systems*, 27(12):2643–2655, 2016. 2

[9] G. Hinton, L. Deng, D. Yu, G.-E. Dahl, A.-R. Mohamed, N. Jaitly, A. Senior, V. Vanhoucke, P. Nguyen, and T. N. Sainath. Deep neural networks for acoustic modeling in speech recognition: The shared views of four research groups. *IEEE Signal Processing Magazine*, 29(6):82–97, 2012. 3

[10] J. Ho, M.-H. Yang, J. Lim, K.-C. Lee, and D.-J. Kriegman. Clustering appearances of objects under varying illumination conditions. In *Proceedings of IEEE International Conference on Computer Vision and Pattern Recognition*, pages 11–18, 2003. 1

[11] P. Ji, M. Salzmann, and H. Li. Efficient dense subspace clustering. In *IEEE Winter conferance on Applications of Computer Vision*, pages 461–468, 2014. 6

[12] P. Ji, T. Zhang, H. Li, M. Salzmann, and I. Reid. Deep subspace clustering networks. In *Neural Information Processing Systems (NIPS)*, 2017. 2, 3, 6, 8

[13] P. Ji, T. Zhang, H. Li, M. Salzmann, and I. Reid. Deep subspace clustering networks. *arXiv preprint arXiv:1709.02508*, 2017. 7

[14] A. Krizhevsky, I. Sutskever, and G. Hinton. Imagenet classification with deep convolutional neural networks. In *Neural Information Processing Systems (NIPS)*, pages 1097–1105, 2012. 3, 4, 6

[15] A. Krizhevsky, I. Sutskever, and G. E. Hinton. Imagenet classification with deep convolutional neural networks. In *Neural Information Processing Systems*, pages 1097–1105, 2012. 1

[16] J. Lezama, Q. Qiu, P. Muse, and G. Sapiro. Ole: Orthogonal low-rank embedding - a plug and play geometric loss for deep learning. In *Proceedings of IEEE International Conference on Computer Vision and Pattern Recognition*, pages 8109–8118, 2018. 2

[17] C.-G. Li and R. Vidal. Structured sparse subspace clustering: A unified optimization framework. In *Proceedings of IEEE International Conference on Computer Vision and Pattern Recognition*, pages 277–286, 2015. 1, 2, 5

[18] C.-G. Li, C. You, and R. Vidal. Structured sparse subspace clustering: A joint affinity learning and subspace clustering framework. *IEEE Transactions on Image Processing*, 26(6):2988–3001, 2017. 1, 2

[19] Q. Li, Z. Sun, Z. Lin, R. He, and T. Tan. Transformation invariant subspace clustering. *Pattern Recognition*, pages 142–155, 2016. 1

[20] G. Liu, Z. Lin, S.-C. Yan, J. Sun, Y. Yu, and Y. Ma. Robust recovery of subspace structures by low-rank representation. *IEEE Transactions on Pattern Analysis and Machine Intelligence*, 35(1):171–184, 2013. 1, 2

[21] G. Liu, Z. Lin, and Y. Yu. Robust subspace segmentation by low-rank representation. In *Proceedings of International Conference on Machine Learning*, pages 663–670, 2010. 1, 2, 6

[22] G. Liu and S. Yan. Latent low-rank representation for subspace segmentation and feature extraction. In *IEEE International Conference on Computer Vision*, pages 1615–1622, 2011. 2, 3

[23] D. Lowe. Distinctive image features from scale-invariant keypoints. *International Journal of Computer Vision*, 20:91–110, 2004. 1

[24] C. Lu, Z. Lin, and S. Yan. Correlation adaptive subspace segmentation by trace lasso. In *Proceedings of IEEE International Conference on Computer Vision*, pages 1345–1352, 2014. 1, 2

[25] C.-Y. Lu, H. Min, Z.-Q. Zhao, L. Zhu, D.-S. Huang, and S.-C. Yan. Robust and efficient subspace segmentation via least squares regression. *Proceedings of European Conference on Computer Vision*, pages 347–360, 2012. 1, 2

[26] B. McWilliams and G. Montana. Subspace clustering of high dimensional data: a predictive approach. *Data Mining and Knowledge Discovery*, 28(3):736–772, 2014. 1

[27] S.-A. Nene, S.-K. Nayar, and H. Murase. Columbia object image library. *Columbia University*, 1996. 6, 7

[28] O. M. Parkhi, A. Vedaldi, A. Zisserman, et al. Deep face recognition. In *BMVC*, volume 1, page 6, 2015. 1

[29] V. M. Patel, H. V. Nguyen, and R. Vidal. Latent space sparse and low-rank subspace clustering. *IEEE Journal of Selected Topics in Signal Processing*, 9(4):691–701, 2015. 2, 3

[30] V.-M. Patel, H. V. Nguyen, and R. Vidal. Latent space sparse subspace clustering. In *Proceedings of IEEE International Conference on Computer Vision*, pages 225–232, Dev 2013. 2, 3

[31] V.-M. Patel. and R. Vidal. Kernel sparse subspace clustering. In *Proceedings of IEEE International Conference on Image Processing*, pages 2849–2853, 2014. 2, 3, 6

[32] X. Peng, J. Feng, S. Xiao, J. Lu, Z. Yi, and S. Yan. Deep sparse subspace clustering. *arXiv preprint arXiv:1709.08374*, 2017. 2

[33] X. Peng, S. Xiao, J. Feng, W. Y. Yau, and Z. Yi. Deep subspace clustering with sparsity prior. In *International Joint Conference on Artificial Intelligence*, pages 1925–1931, 2016. 2, 3

[34] X. Peng, Z. Yu, Z. Yi, and H. Tang. Constructing the l_2-graph for robust subspace learning and subspace clustering. *IEEE Transactions on Cybernetics*, 47(4):1053–1066, 2017. 1, 2

[35] X. Qi, C.-G. Li, G. Zhao, X. Hong, and M. Pietikainen. Dynamic texture and scene classification by transferring deep image features. *Neurocomputing*, 171:1230–1241, 2016. 3

[36] X. Qi, R. Xiao, C.-G. Li, Y. Qiao, J. Guo, and X. Tang. Pairwise rotation invariant co-occurrence local binary pattern. *IEEE Transactions on Pattern Analysis and Machine Intelligence*, 36(11):2199–2213, 2014. 1

[37] F.-S. Samaria and A.-C. Harter. Harter, a.: Parameterisation of a stochastic model for human face identification. In *Proceedings of the Second IEEE Workshop on Applications of Computer Vision*, pages 138–142, 1994. 6, 7

[38] R. Shankar, T. Roberto, R. Vidal, and Y. Ma. Motion segmentation in the presence of outlying, incomplete, or corrupted trajectories. *IEEE Transactions on Pattern Analysis and Machine Intelligence*, 32(10):1832–1845, 2010. 1

[39] C. Tomasi and T. Kanade. Shape and motion from image streams under orthography: a factorization method. *International Journal on Computer Vision*, 9(2):137–154, 1992. 1

[40] R. Vidal. Subspace clustering. *IEEE Signal Processing Magazine*, 28(2):52–68, 2011. 1

[41] R. Vidal and P. Favaro. Low rank subspace clustering (lrsc). *Pattern Recognition Letters*, 43:47–61, 2014. 6

[42] R. Vidal, Y. Ma, and S. Sastry. Generalized Principal Component Analysis (GPCA). *IEEE Transactions on Pattern Analysis and Machine Intelligence*, 27(12):1–15, 2005. 1

[43] Y. X. Wang, H. Xu, and C. Leng. Provable subspace clustering: when lrr meets ssc. In *Neural Information Processing Systems (NIPS)*, pages 64–72, 2013. 2

[44] S. Xiao, M. Tan, D. Xu, and Z.-Y. Dong. Robust kernel low-rank representation. *IEEE Transactions on Neural Networks and Learning Systems*, 27(11):2268–2281, 2016. 2, 3

[45] B. Xin, Y. Wang, W. Gao, and D. Wipf. Building invariances into sparse subspace clustering. *IEEE Transactions on Signal Processing*, 66(2):449–462, 2018. 2

[46] H. N. W. Yang, F. Shen, and C. Sun. Kernel low-rank representation for face recognition. *Neurocomputing*, 155:32–42, 2015. 2, 3

[47] C. You, C. Li, D. P. Robinson, and R. Vidal. Scalable exemplar-based subspace clustering on class-imbalanced data. In *Proceedings of European Conference on Computer Vision*, September 2018. 2

[48] C. You, C.-G. Li, D. Robinson, and R. Vidal. Oracle based active set algorithm for scalable elastic net subspace clustering. In *Proceedings of IEEE International Conference on Computer Vision and Pattern Recognition*, pages 3928–3937, 2016. 1, 2

[49] C. You, D. Robinson, and R. Vidal. Scalable sparse subspace clustering by orthogonal matching pursuit. In *Proceedings of IEEE International Conference on Computer Vision and Pattern Recognition*, pages 3918–3927, 2016. 6

[50] P. Zhou, Y. Hou, and J. Feng. Deep adversarial subspace clustering. In *Proceedings of IEEE International Conference on Computer Vision and Pattern Recognition*, June 2018. 2, 3